Electronic Supplementary Material (ESI) for Journal of Materials Chemistry A.

Electronic Supporting Information

Chemical Insights into Electrophilic Fluorination of SnO_2 for Photoelectrochemical Applications

Gaurav Bahuguna [#] *Mohit Verma*[#] *and Ritu Gupta**
Department of Chemistry, Indian Institute of Technology Jodhpur,
Jodhpur, Rajasthan-342037, India

[#]Both authors contributed equally.
*Corresponding Author: Prof. Ritu Gupta (ritu@iitj.ac.in)

Table of Contents:

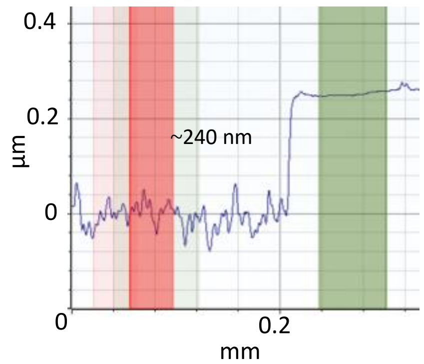

Figure S1: F-SnO_2 film thickness measurement by surface profilometer.

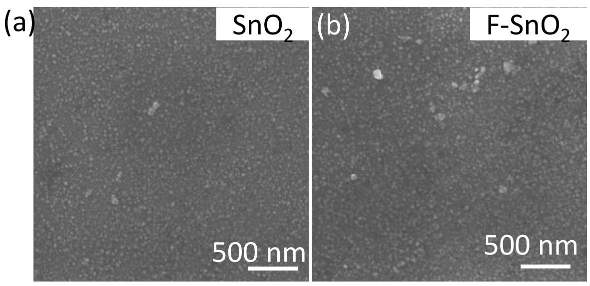

Figure S2: SEM images of (a) SnO_2 and (b) F-SnO_2 films.

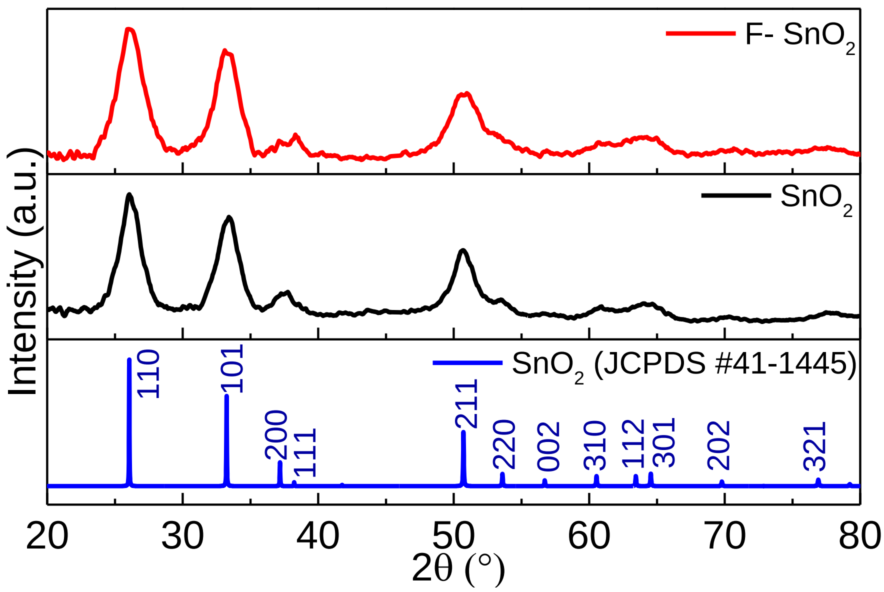

Figure S3: XRD patterns of SnO_2 and F-SnO_2 films.

Table S1: Crystallite size of SnO_2 and F-SnO_2 film

Film	Crystallite size (D, nm)
SnO_2	4.08
F-SnO_2	3.81

$D = k\lambda/\beta cos\theta$ k, λ, β and θ are shape factor constant, wavelength of X-ray, full width at half maximum (FWHM) and Bragg angle of 110 diffraction.

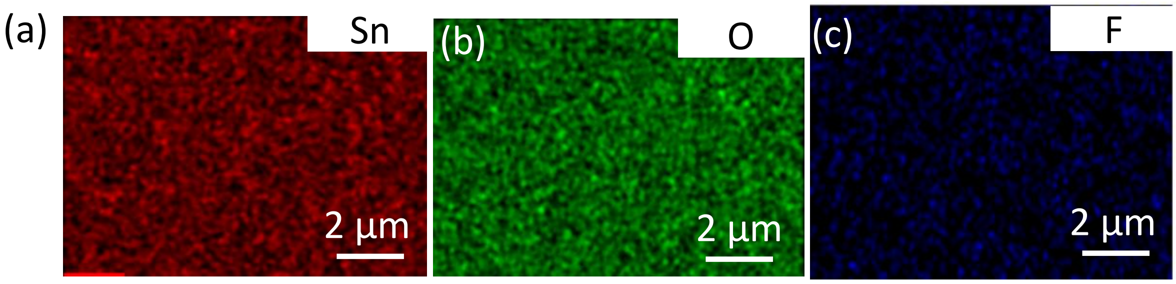

Figure S4: Energy dispersive X-ray (EDX) mapping of (a) Sn, (b) O, and (c) F of F-SnO_2 film.

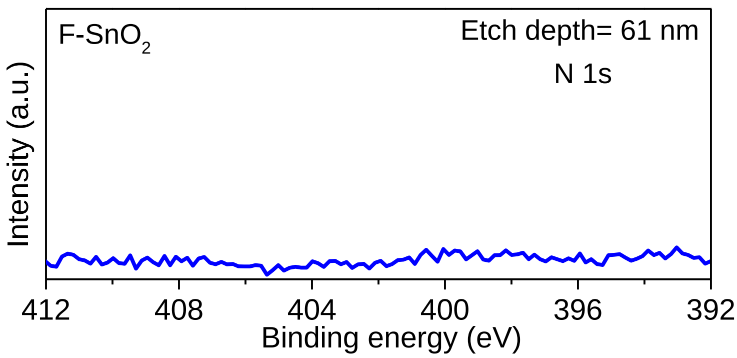

Figure S5: High resolution N1s XPS spectrum of F-SnO_2 film at 32 nm etch depth.

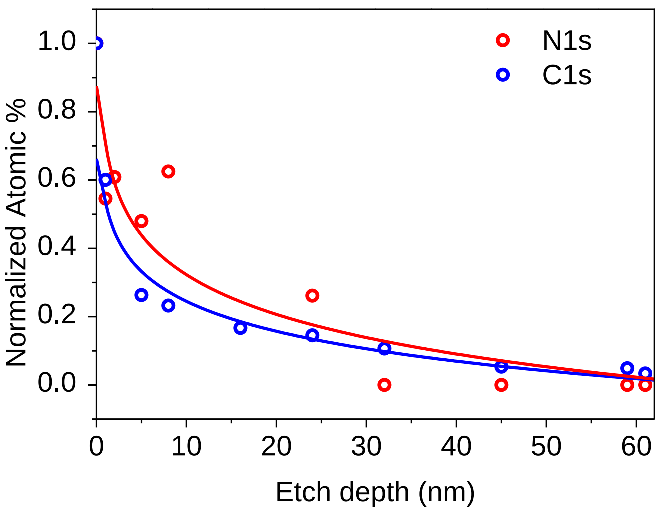

Figure S6: Variation in N1s and C1s along the depth of F-SnO_2 film.

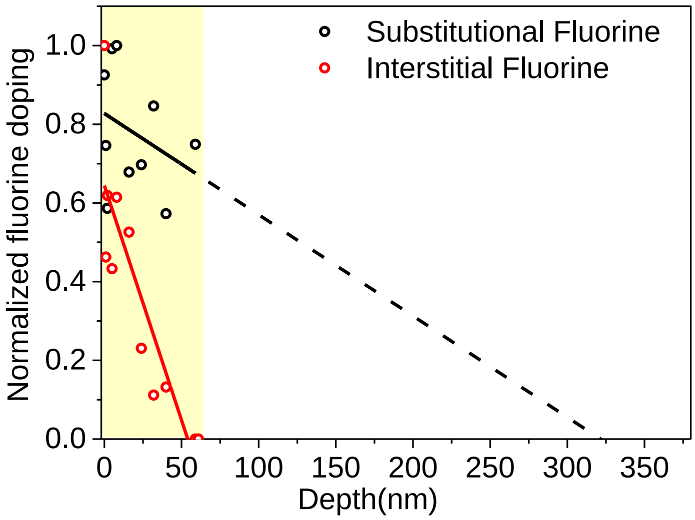

Figure S7: Variation in substitutional and interstitial fluorine percentage present in F-SnO_2 lattice along with the linearly fitted extrapolated plots for calculation of diffusion coefficient.

Table S2: XPS analysis of O1s for SnO_2 and F-SnO_2 films.

	O-Sn^{4+}		**O-Sn^{2+}**		**O_{Chem}**		**O-Sn^{2+}/ O-Sn^{4+}**	**Total O1s**	**Oxygen defect ratio**	**Oxygen Defects**
	Peak position (eV)	Area under the curve	Peak position (eV)	Area under the curve	Peak position (eV)	Area under the curve	-	**(%)**	-	**(%)**
SnO_2	530.47	14638.1	531.48	12528.1	532.83	1548.2	0.85	40.1	0.43	17.24
F-SnO_2	530.36	15438.7	531.93	1770.39	532.82	1413.08	0.07	35.75	0.095	3.39

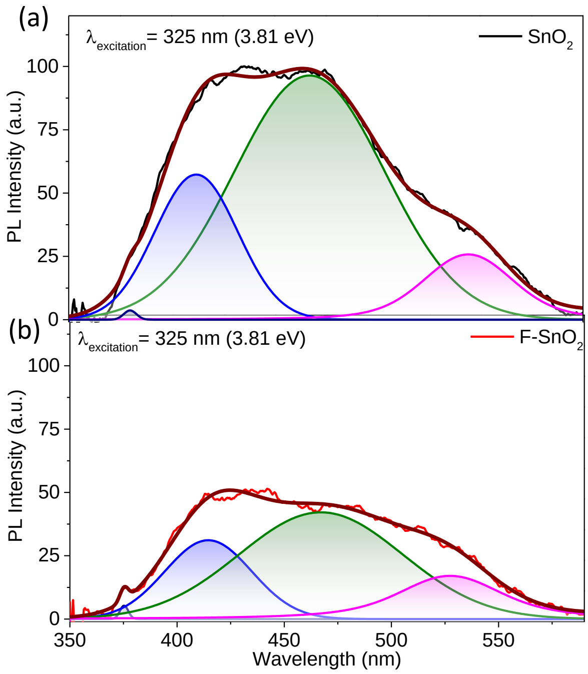

Figure S8: Photoluminescence (PL) spectra of (a) SnO_2 and (b) F-SnO_2 films at an excitation wavelength of 325 nm.

Photoluminescence (PL) measurements of SnO_2 film before and after fluorination can provide information about the defects and oxygen vacancies.PL spectrum of SnO_2 film shows a broad emission peak which can be deconvoluted further into four peaks (Figure S8a). The peak around ~379 nm is assigned to the near band edge emission,[1] while the second peak at ~410 nm is due to the transition from the conduction band to the intermediate donor levels (V_o^{++}) created by oxygen vacancy sites near the valence band.[2] The third peak at ~463 nm corresponds to the transitions between the acceptor levels created below the conduction band (V_o^0) to the oxygen defect sites near valence band (V_o^{++})[2] and fourth peak at ~537 nm to the structural defects or polycrystallinity.[3] Upon fluorination, PL spectrum of F-SnO_2 film does not shows any significant shift in the peak positions (Figure S8b) although a significant decrease in the PL peak intensities is observed due to reduction in oxygen defects (V_o^{++} and V_o^0) present in the SnO_2 film.

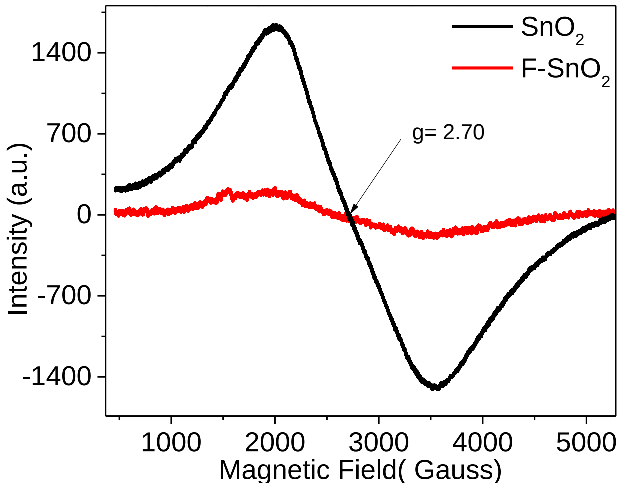

Figure S9: Electron Paramagnetic Resonance (EPR) spectra of pristine SnO_2 and F-SnO_2 films.

To further probe the effect of fluorination on the oxygen vacancies, EPR measurement is performed on the powder samples scraped from corresponding thin films. The g-factor is calculated using the equation g = hγ/B, where h is the Planck's constant (6.626 × 10^{-27} erg-s/cycle), γ is the frequency (Hz), B is the Bohr's magneton (9.274 × 10^{-21}) and H is the static magnetic field (gauss). The EPR spectra with significant intensity and g=2.7 signify the presence of oxygen vacancies (V_o^{++}) as paramagnetic centres in SnO_2 powder (Figure S9). Interestingly, F-SnO_2 exhibits a significant reduction in the signal intensity indicating the reduction of oxygen vacancies.

Table S3: Impedance parameters derived by fitting the Nyquist plots.

Film	Temperature (°C)	Contact Resistance R_C (Ω)	Bulk Resistance R_B (kΩ)	Q $\times10^{-12}$ (F $s^{\alpha-1}$)	α
SnO_2	25	2572.5	1598.80	3.5	1.03
	50	2252.8	980.90	2.5	1.05
	75	2511.2	470.44	1.9	1.07
	100	4738.5	108.04	2.2	1.09
F-SnO_2	25	1861.0	7.04	28	1.05
	50	2711.9	4.89	2.5	1.18
	75	2383.9	4.30	6.2	1.13
	100	1974.0	3.99	0.3	1.04

$Z_{CPE} = 1/(j\omega)^{\alpha}$ Q is a nonideal capacitance and has units of F $s^{\alpha-1}$ and α is an ideality factor

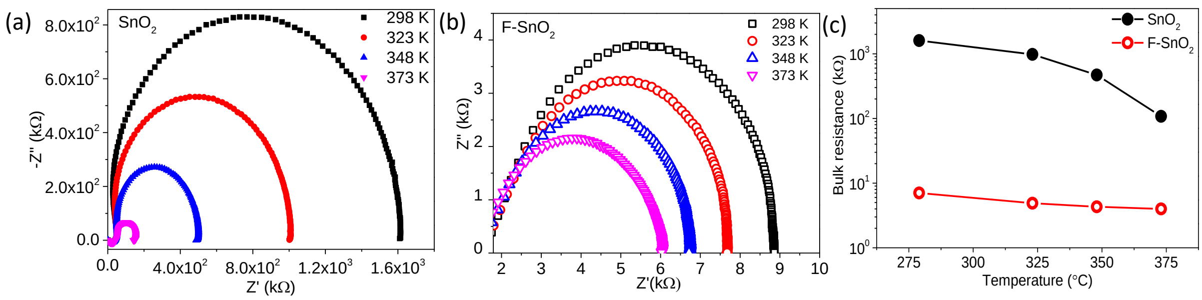

Figure S10: Nyquist plots of (a) SnO_2 and (b) F-SnO_2 films at different temperatures. (c) Bulk resistance values of SnO_2 and F-SnO_2 films obtained from the Nyquist plot at different temperatures.

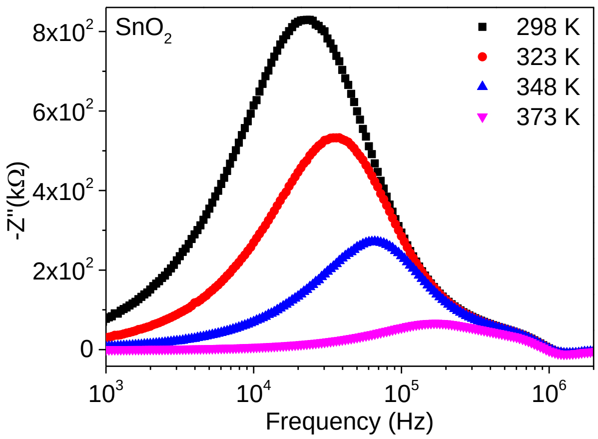

Figure S11: Imaginary part of impedance (-Z″) as a function of frequency of SnO_2 film at different temperatures.

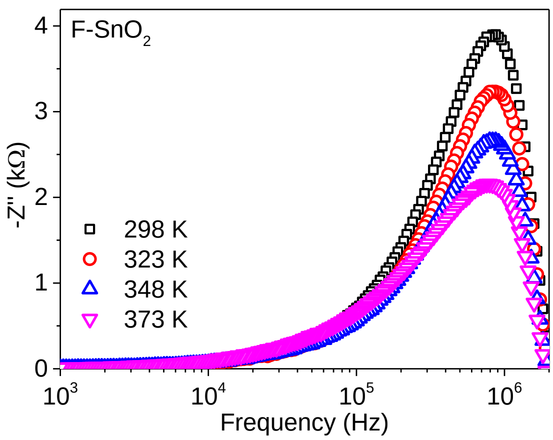

Figure S12: Imaginary part of impedance (-Z″) as a function of frequency of F-SnO_2 film at different temperatures.

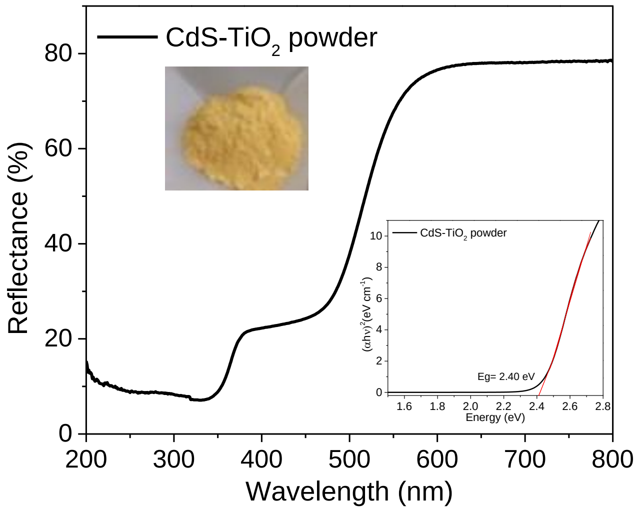

Figure S13: UV-Vis diffuse reflectance spectrum and the corresponding Tauc plot of CdS-TiO_2 (Sensitizer, S*) powder.

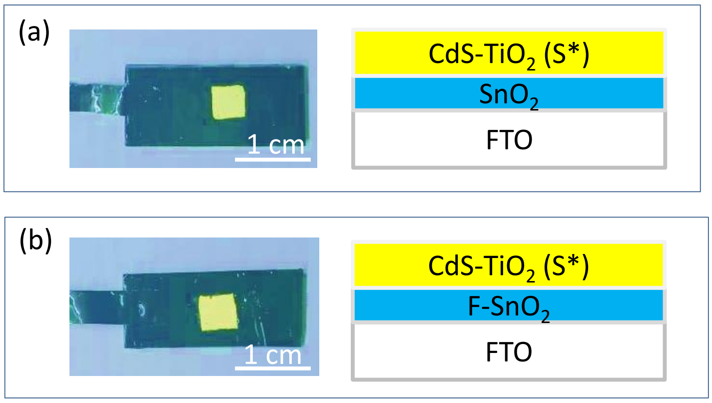

Figure S14: Photograph and geometry of (a) S*/SnO_2 and (b) S*/F-SnO_2 electrodes.

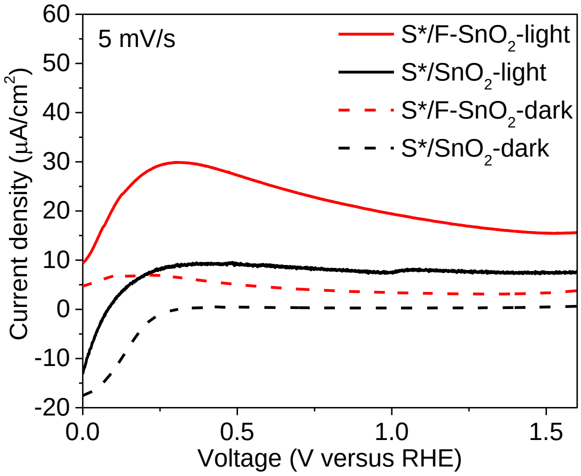

Figure S15: I-V characteristics of S^*/SnO_2 and $S^*/F\text{-}SnO_2$.

Table S4: EIS parameters derived by fitting the Nyquist plots.

Electrodes	$R_s(\Omega)$	$R_{CT}(\Omega)$	C1 (F)	$R_{rr}(k\Omega)$	C2 (F)
$S^*/SnO_2/FTO$	3.6	13.4	5.5×10^{-8}	10.7	4.1×10^{-7}
$S^*/F\text{-}SnO_2/FTO$	3.3	12.82	6.4×10^{-8}	6.8	2.7×10^{-7}

References:

1 M. Bhatnagar, V. Kaushik, A. Kaushal, M. Singh and B. R. Mehta, *AIP Adv.*, 2016, **6**, 095321.
2 A. Kar, S. Kundu and A. Patra, *J. Phys. Chem. C*, 2011, **115**, 118–124.
3 J. K. Yang, H. L. Zhao, J. Li, L. P. Zhao, J. J. Chen and B. Yu, *Acta Mater.*, 2014, **62**, 156–161.